Available online at www.sciencedirect.com
SCIENCE DIRECT
ELSEVIER
International Journal for Parasitology 35 (2005) 193–206
INTERNATIONAL Journal for PARASITOLOGY
www.parasitology-online.com

Ultrastructural differentiation of *Toxoplasma gondii* schizonts (types B to E) and gamonts in the intestines of cats fed bradyzoites

C.A. Speer[a,b], J.P. Dubey[c,*]

[a]*Department of Forestry, Wildlife and Fisheries, Agricultural Experiment Station, Institute of Agriculture, The University of Tennessee, Knoxville, TN 37920, USA*
[b]*Center for Bison and Wildlife Health, Department of Veterinary Molecular Biology, Montana State University, Bozeman, MT 59717, USA*
[c]*US Department of Agriculture, Agricultural Research Service, Animal and Natural Resources Institute, Animal Parasitic Diseases Laboratory, BARC-East, Building 1001, Beltsville, MD 20705-2350, USA*

Received 2 September 2004; received in revised form 19 October 2004; accepted 3 November 2004

Abstract

The ultrastructural characterisitics of four types of *Toxoplasma gondii* schizonts (types B, C, D and E) and their merozoites, microgamonts and macrogamonts were compared in cats killed at days 1, 2, 4 and 6 after feeding tissues cysts from the brains of mice. Schizonts, merozoites and gamonts contained most of the ultrastructural features characteristic of the phylum Apicomplexa. All four types of schizonts developed within enterocytes or intraepithelial lymphocytes. Occasionally, type B and C schizonts developed within enterocytes that were displaced beneath the epithelium into the lamina propria. Type D and E schizonts and gamonts developed exclusively in the epithelium. Tachyzoites occurred exclusively within the lamina propria. Type B schizonts formed merozoites by endodyogeny, whereas types C to E developed by endopolygeny. The parasitophorous vacuoles surrounding type B and C schizonts consisted of a single membrane, whereas those surrounding types D and E schizonts were comprised of two to four electron-dense membranes. The parasitophorous vacuole of type B schizonts had an extensive tubulovesicular membrane network (TMN); the TMN was reduced or absent in type C schizonts and completely absent in types D and E schizonts and gamonts. Type B merozoites were ultrastructurally similar to tachyzoites, except that they were slightly larger. Type C merozoites exhibited a positive periodic acid-Schiff reaction by light microscopy and ultrastructurally contained amylopectin granules. Rhoptries were labyrinthine in type B merozoites but were electron-dense in types C–E. The development of microgamonts, macrogamont and oocysts is also described.
Published by Elsevier Ltd on behalf of Australian Society for Parasitology Inc.

Keywords: *Toxoplasma gondii*; Cats; Schizonts; Intestine; Gamonts; Ultrastructure; Types B–E; Merozoites

1. Introduction

Felids are the only definitive hosts for *Toxoplasma gondii* (Frenkel et al., 1970). Cats shed oocysts after ingesting any of the three infectious stages of *T. gondii*, i.e. tachyzoites, bradyzoites, and sporozoites. Prepatent periods (time interval to the shedding of oocysts after the initial inoculation) and frequency of oocyst shedding vary according to the stage of *T. gondii* ingested (Frenkel et al., 1970; Dubey and Frenkel, 1976; Freyre et al., 1989; Dubey, 1996; Dubey, 2001). Prepatent periods are 3–10 days after ingesting tissue cysts and 18 days or more after ingesting tachyzoites or oocysts. Less than 50% of cats shed oocysts after ingesting tachyzoites or oocysts whereas nearly all cats shed oocysts after ingesting tissue cysts (Dubey and Frenkel, 1976). The developmental stages of *T. gondii* in the gut of cats after ingesting tachyzoites and oocysts are unknown.

Dubey and Frenkel (1972) described the development of asexual enteroepithelial stages (schizonts) of *T. gondii* based on light microscopic observations of cats killed 1–15 days after feeding tissue cysts. After the ingestion of tissue cysts by cats, the tissue cyst wall is dissolved by proteolytic enzymes in the stomach and the small intestine. The released bradyzoites penetrate the epithelial cells of the small intestine and initiate the development of numerous generations of *T. gondii*. Five morphologically distinct types

* Corresponding author. Tel.: +1 301 504 8128; fax: +1 301 504 9222.
E-mail address: jdubey@anri.barc.usda.gov (J.P. Dubey).

0020-7519/$30.00 Published by Elsevier Ltd on behalf of Australian Society for Parasitology Inc.
doi:10.1016/j.ijpara.2004.11.005

of *T. gondii* develop in intestinal epithelial cells before gametogony begins (Dubey and Frenkel, 1972). These stages were designated types A to E instead of generations because there were several generations within each *T. gondii* type. Other researchers reported only one morphologic type of schizont in the intestine of the cat but they studied tissues of cats five or more days after feeding tissue cysts (Sheffield, 1970; Hutchison et al., 1971, Piekarski et al., 1971; Ferguson et al., 1974; Overdulve, 1978). Thus, the ultrastructure of type A to C schizonts is unknown. In the present paper, we report the unique ultrastuctural features of type B to E schizonts and merozoites, gamonts and early stages of oocysts of *T. gondii*.

2. Materials and methods

Six newborn kittens (1- to 6-days old) raised in captivity (Dubey, 1995) were inoculated orally via a stomach tube tissue cysts of *T. gondii*. Kittens 1–5 were given the wallaby 1 strain of *T. gondii* isolated in 1996 from the brain of a naturally infected *Macrops eugenii* (J. Dubey, unpubl. obs.). This strain was cycled between mice and cats only twice to obtain oocysts and tissue cysts. It is genetic Type III and it produces many tissue cysts. Tissue cysts were separated from brain tissue of chronically infected mice by a Percoll gradient (Cornelissen et al., 1981).

Kitten 1 was given Percoll separated tissue cysts and euthanised 24 h later. Kittens 2–5 were 5-day-old littermates and were given both Percoll isolated tissue cysts as well as mouse brain homogenate in two meals with a 4 h interval. Kitten 2 was euthanised 46 h p.i. and kitten 3 was euthanised 52 h p.i. Most of the ultrastructural study is based on these three kittens. Kittens 4 and 5 were given mouse brain homogenates and euthanised 4 and 6 days later. Kitten 6 was given Percoll separated tissue cysts of the VEG strain of *T. gondii* (Type III strain, Dubey et al., 1996) and was euthanised 8 h later. All experiments were approved by the Institutional Animal Care Committee.

The small intestine (~75 cm long) was divided into five equal segments, slit open, and small pieces from segments one and two were fixed in modified Karnovsky's; remaining intestine was fixed in 10% neutral buffered formalin. Formalin-fixed tissues were embedded in paraffin, and 5 μm sections were examined microscopically after staining with haematoxylin and eosin (H&E). Selected samples from heavily infected areas were embedded in methacrylate and 3 μm sections examined microscopically after staining with H&E.

Pieces of the small intestine fixed in Karnovsky's modified fixative were prepared for transmission electron microscopy (TEM) as described previously (Speer et al., 1997), except that they were prestained with 1% (w/v) phosphotungstic acid and 1% (w/v) uranyl acetate in 70% ethanol. Ultrathin sections were examined with a JEOL 100 CX scanning-transmission electron microscope.

3. Results

3.1. Tachyzoites

Tachyzoites, which were seen throughout the study, occurred exclusively in the lamina propria at 1–6 days p.i. They infected neutrophils, lymphocytes, capillary and lymphatic endothelial cells, macrophages, fibroblasts and occasionally eosinophils and mast cells. Tachyzoites were situated in a prominent parasitophorous vacuole (PV) that contained a well-developed tubulovesicular membrane network (TMN) and developed exclusively by endodyogeny. They measured 4.7×2.1 μm ($n = 10$) in size by TEM.

3.2. Schizonts

Light microscopy revealed that schizonts were usually located between the host cell nucleus and the brush border of enterocytes (Fig. 1), except for some that occurred within enterocytes that were displaced into the lamina propria (Fig. 1H). Type B schizonts multiplied by endodyogeny, whereas types C to E multiplied by endopolygeny in which multiple nuclear divisions occurred followed by merozoites budding at the schizont surface (Fig. 1H). Type B, D and E schizonts were PAS-negative, whereas type C schizonts were PAS-positive (Fig. 1D). Type B merozoites frequently remained within the same parasitophorous vacuole (PV) in which they had developed (Fig. 1C and G). By light microscopy type B and C schizonts were located below the host cell nucleus (hcn) whereas types D and E were always above the hcn.

TEM revealed that all schizonts, merozoites and tachyzoites contained organelles that are characteristically found in these stages for most apicomplexans including conoid, rhoptries, micronemes, nucleus and nucleolus, plasmalemma, inner membrane complex, subpellicular microtubules, precondoidal rings (apical rings), polar rings, micropores, Golgi complex, multiple-membrane bound vacuole (Golgi adjunct or apicoplast), endoplasmic reticulum, numerous ribosomes, lipid bodies, dense granules, mitochondria and amylopectin granules (Figs. 2–7).

Each type of schizont and merozoite differed in time and duration of occurrence and contained certain unique ultrastructural features. Host cells also exhibited ultrastructural differences in the structure of the PV.

3.2.1. Type B schizonts

Type B schizonts were situated within a PV consisting of a well developed TMN and prominent PV with a thin parasitophorous vacuolar membrane (PVM). Merozoites multiplied exclusively by endodyogeny and most were in various stages of multiplication (Fig. 2A and C). Ultrastructurally, type B merozoites were similar to tachyzoites except that they occurred only in enterocytes and were larger, measuring 5.8×2.9 μm ($n = 10$) in size. They had only a few small amylopectin granules and their rhoptries

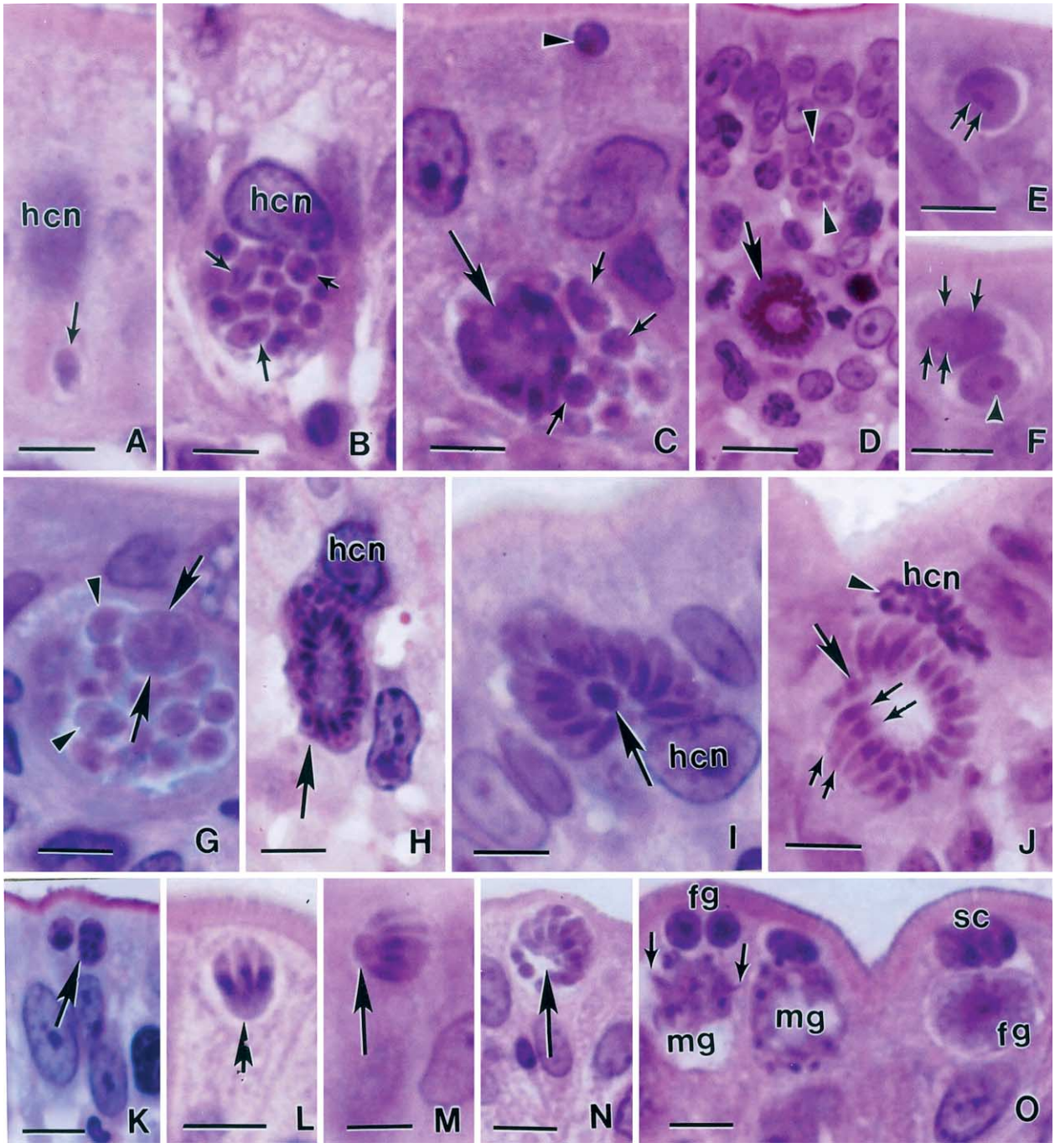

Fig. 1. Enteroepithelial stages of *Toxoplasma gondii* in enterocytes of the small intestine of cats fed tissues cysts. All slides were stained with haematoxylin and eosin except D, H and K, which were stained with periodic acid-Schiff reaction counter stained with haematoxylin. All figures are oriented with the intestinal lumen at the top. Bars represent 5 μm. (A) Bradyzoite (arrow) below the host cell nucleus (hcn), 8 h p.i. (B) Type B schizont with several organisms (arrows) dividing into two, 42 h p.i. (C) Type B schizont with a multinucleated mass (large arrow) and individual zoites (small arrows) in the same PV. An uninucleate parasite (arrowhead) is located under the microvillar border, 42 h p.i. (D) Type B PAS-negative schizont (arrowheads) and a PAS-positive type C schizont (arrow), 42 h p.i. (E) An organism (probably type C schizont) with a large nucleus with two prominent nucleoli (arrows), 24 h p.i. (F) Two organisms, presumably type C in the same PV, one with a large nucleus (arrowhead) and the other with two nucleoli (arrows); 24 h p.i. (G) A multinucleated mass (arrows) and several type B merozoites (arrowheads), 42 h p.i. (H) Multinucleated type C schizont in the lamina propria in an epithelial cell; 42 h p.i. (I) Type C schizont with residual body (arrow), 42 h p.i. (J) Type C schizont (large arrow) with peripherally arranged merozoites (small arrows). The hcn is dividing (arrowhead), 42 h p.i. (K) Type D schizont (arrow) with multiple nuclei, 42 h p.i. (L) Type D schizont with merozoites budding from a residual body (arrow), 42 h p.i. (M) Type D schizont (arrow) with a residual body (arrow), 42 h p.i. (N) Type E schizont (arrow), 6 days p.i. (O) Male gamonts (mg) and female gamonts (fg), and a schizont (sc), arrows point to microgametes, 6 days p.i.

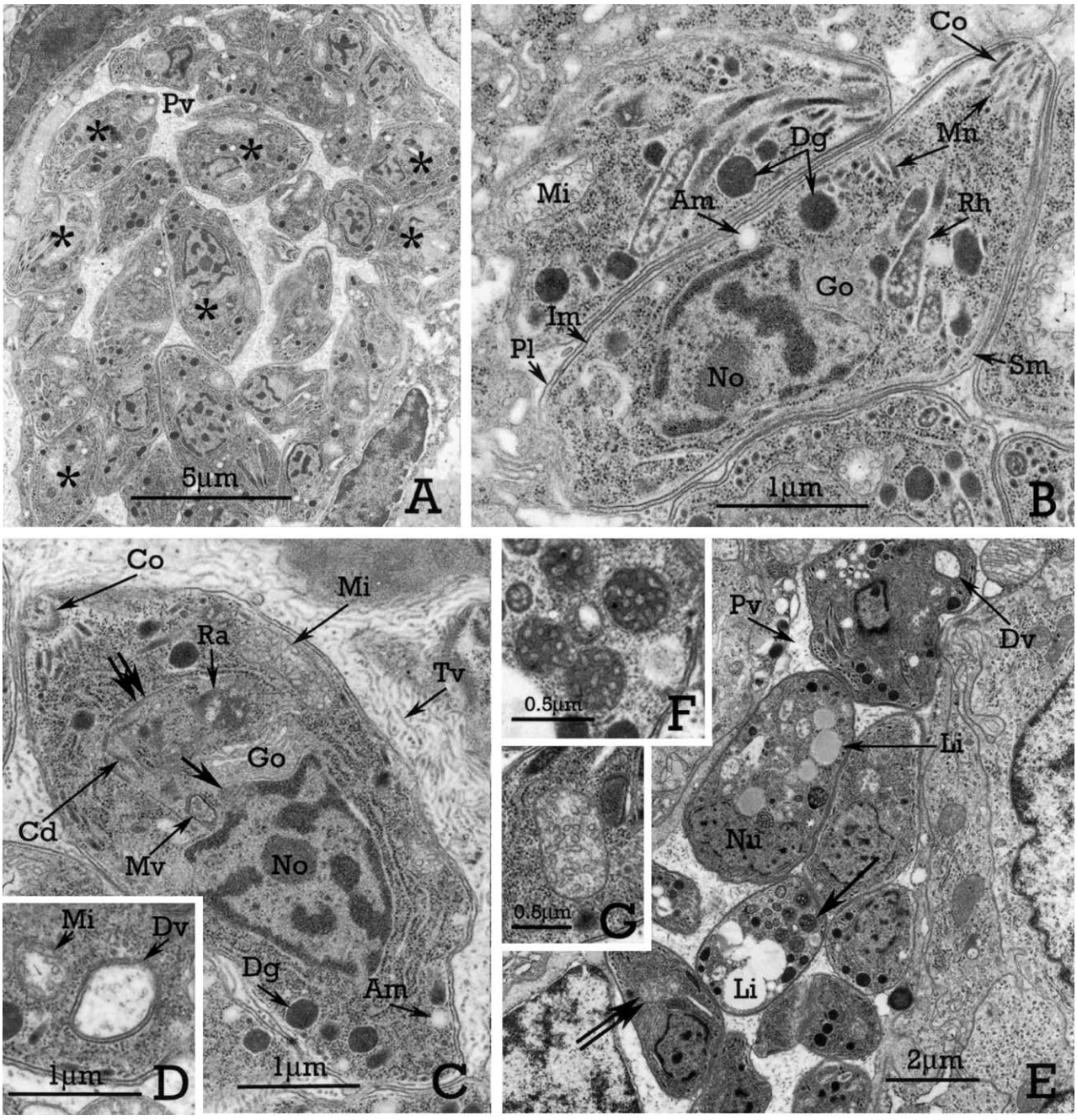

Fig. 2. Transmission electron micrograph of type B schizonts, 46 h p.i. (A) Type B schizont with merozoites, many of which are in various stages of endodyogeny (*). The parasitophorous vacuole (Pv) contains an extensive tubulovesicular membrane network, 46 h p.i. (B) Type B merozoites showing various organelles including labyrinthine rhoptries (Rh); Am, amylopectin granule; Co, conoid; Dg, dense granule; Go, Golgi complex; Im, inner membrane complex of pellicle; Mn, microneme; No, nucleolus; Pl, plasmalemma of pellicle; Sm, subpellicular microtubule. (C) Higher magnification of a merozoite in (A) undergoing endodyogeny; single arrow shows spindle polar cone of dividing nucleus; double arrows show inner membrane complex of daughter zoite developing internally; Am, amylopectin; Cd, conoid of developing zoite; Co, conoid; Dg, dense granule; Go, Golgi complex; Mi, mitochondrion; Mv, multiple-membrane bound vacuole; No, nucleolus; Ra, rhoptry anlagen; Tv, tubule of tubulovesicular membrane network. (D) Higher magnification of large form at top of (E) showing typical mitochondrion (Mi) and an unusual double-membrane bound vacuole (Dv). (E) Merozoites and several large uninucleate schizonts developing within the same parasitophorous vacuole; note that the uninucleate schizonts contain large nuclei (Nu), numerous lipid bodies (Li), mitochondria with electron-dense matrices (single arrow) as well as typical mitochondria; typical mitrochondria occur in merozoites (double arrow); Pv, parasitophorous vacuole. (F) Higher magnification of mitochondria with dense matrix shown by single arrow in large form in (E). (G) Higher magnification of normal mitochondrion shown by double arrow in merozoite in (E).

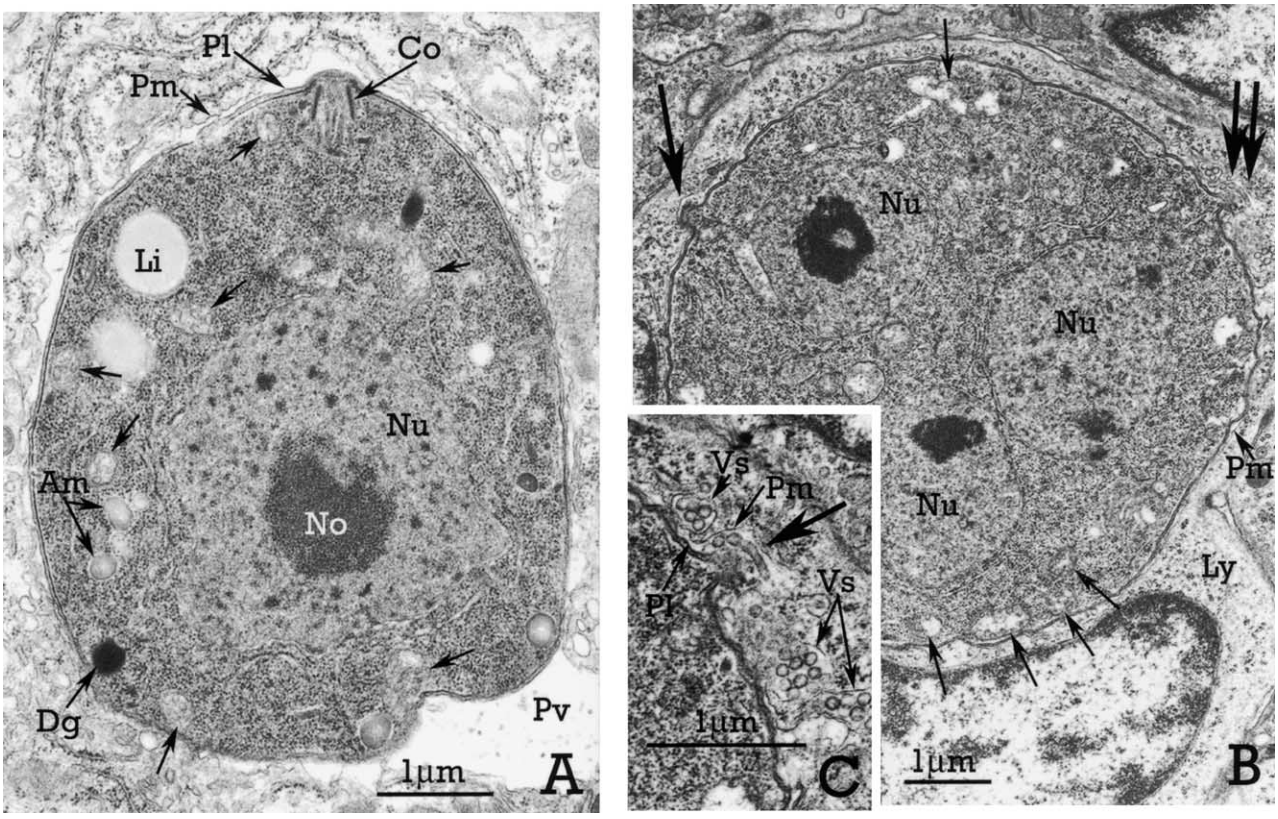

Fig. 3. Transmission electron micrograph of (A) an uninucleate parasite and (B) an intermediate schizont developing into type C schizonts, 1 day p.i. (A) Uninucleate schizont in early stage of developing into a type C schizont showing a large nucleus (Nu) and nucleolus (No), scattered amylopectin granules (Am), conoid (Co), dense granule (Dg) and numerous, small mitochondria (single arrows) most of which are located immediately beneath the pellicle; the parasitophorous vacuole (Pv) contains remnants of the tubulovesicular membrane network; pl, plasmalemma of uninucleate schizont; Pm, parasitophorous vacuolar membrane. (B) Intermediate type C schizont in an intraepithelial lymphocyte (Ly); schizont shows three nuclei (Nu) and numerous small mitochondria (single arrows); protrusions from the schizont pellicle indent (single and double arrows) the parasitophorous vacuolar membrane (Pm). (C) Higher magnification of protrusion (arrow) of schizont pellicle in (B); note that vesicles appear to have formed from the schizont plasmalemma (Pl) and the host cell cytoplasm contains several vacuoles (Vs) containing these small vesicles.

were labyrinthine. Some merozoites remained within the same PV and transformed into larger forms with multiple nuclei. These multinucleate forms evidently were early stages of developing type C schizonts as observed by light microscopy but type C schizonts that produced merozoites within the original PV were not observed ultrastructurally. The large multinucleate forms had numerous lipid bodies, a prominent double-membrane bound vacuole and mitochondria with electron-dense matrices as well as typical mitochondria with moderately electron-dense matrices (Fig. 2D–F). Merozoites within the same PV as the large forms contained typical mitochondria, few lipid bodies and no double-membrane bound vacuoles (Fig. 2E and G).

3.2.2. Type C schizonts

Type C schizonts multiplied by endopolygeny either in enterocytes or intraepithelial lymphocytes (Figs. 3 and 4). Uninucleate schizonts (Fig. 3A) that appeared destined to form type C schizonts were located in a PV that contained a reduced TMN (Fig. 3A) with most of the PVM closely associated with the schizont pellicle (Fig. 3A). Type C uninucleate schizonts were spheroid, contained few micronemes, few dense granules, several lipid bodies and small mitochondria, and few amylopectin granules (Fig. 3A). Early intermediate type C schizonts contained several nuclei with prominent nucleoli, many small mitochondria located immediately beneath the pellicle, and several pellicular protrusions that indented the PVM (Fig. 3B and C). The pellicular protrusions gave rise to small vesicles, 85 nm in diameter, which became encased in a vacuole, 200–550 nm in diameter, in the host cell cytoplasm (Fig. 3C). Some of the large vacuoles contained as many as 15 vesicles in a single section. The PV contained no TMN and the PVM was closely associated with the parasite pellicle (Fig. 3B).

Advanced intermediate schizonts contained merozoites that developed internally by endopolygeny (Fig. 4A) in which two merozoites were formed in association with each pole of a single nucleus undergoing the last division. Eventually, merozoites budded from the surface of the schizont leaving a residual body that measured

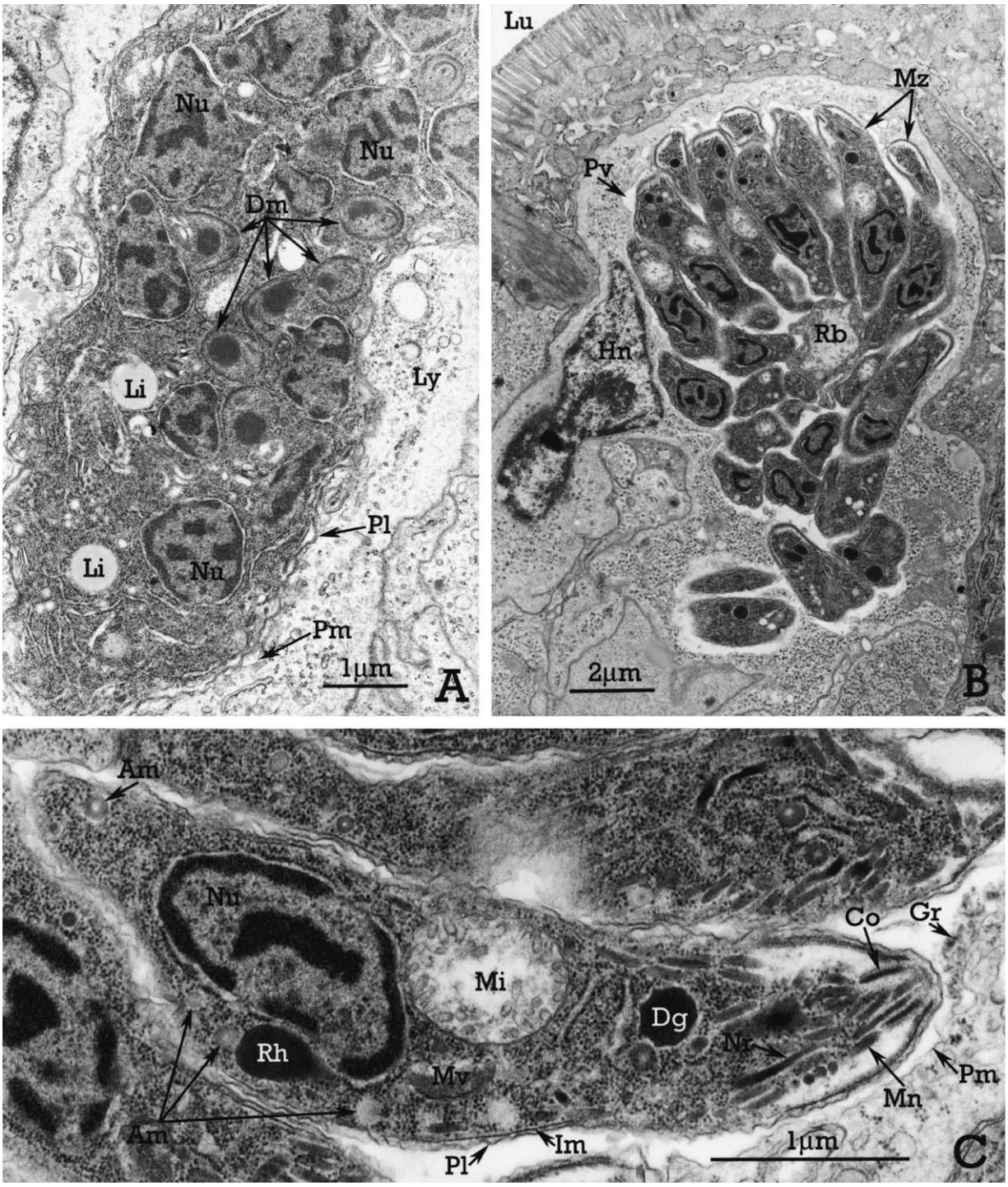

Fig. 4. Transmission electron micrograph of type C schizonts (A and B) and merozoites (C) in intraepithelial lymphocytes (Ly); 46 h p.i. (A) Intermediate schizont in an early stage of endopolygeny; note nuclei (Nu), developing merozoites (Dm), lipid bodies (Li) and parasitophorous vacuolar membrane (Pm) closely associated with the schizont plasmalemma (Pl). (B) Nearly mature type C schizont with merozoites (Mz) budding from a centrally located residual body (Rb); note narrow parasitophorous vacuole (Pv); Hn, host cell nucleus; Lu, lumen of intestinal tract. (C) Higher magnification of type C merozoite in (B) showing scattered amylopectin granules (Am), electron-dense rhoptry (Rh), large mitochondrion (Mi), conoid (Co), dense granule (Dg), granules (Gr) in the parasitophorous vacuole, inner membrane complex (Im), micronemes (Mn), multiple-membrane bound vacuole (Mv), neck of rhoptry (Nr), plasmalemma (Pl) of merozoite and parasitophorous vacuolar membrane (Pm).

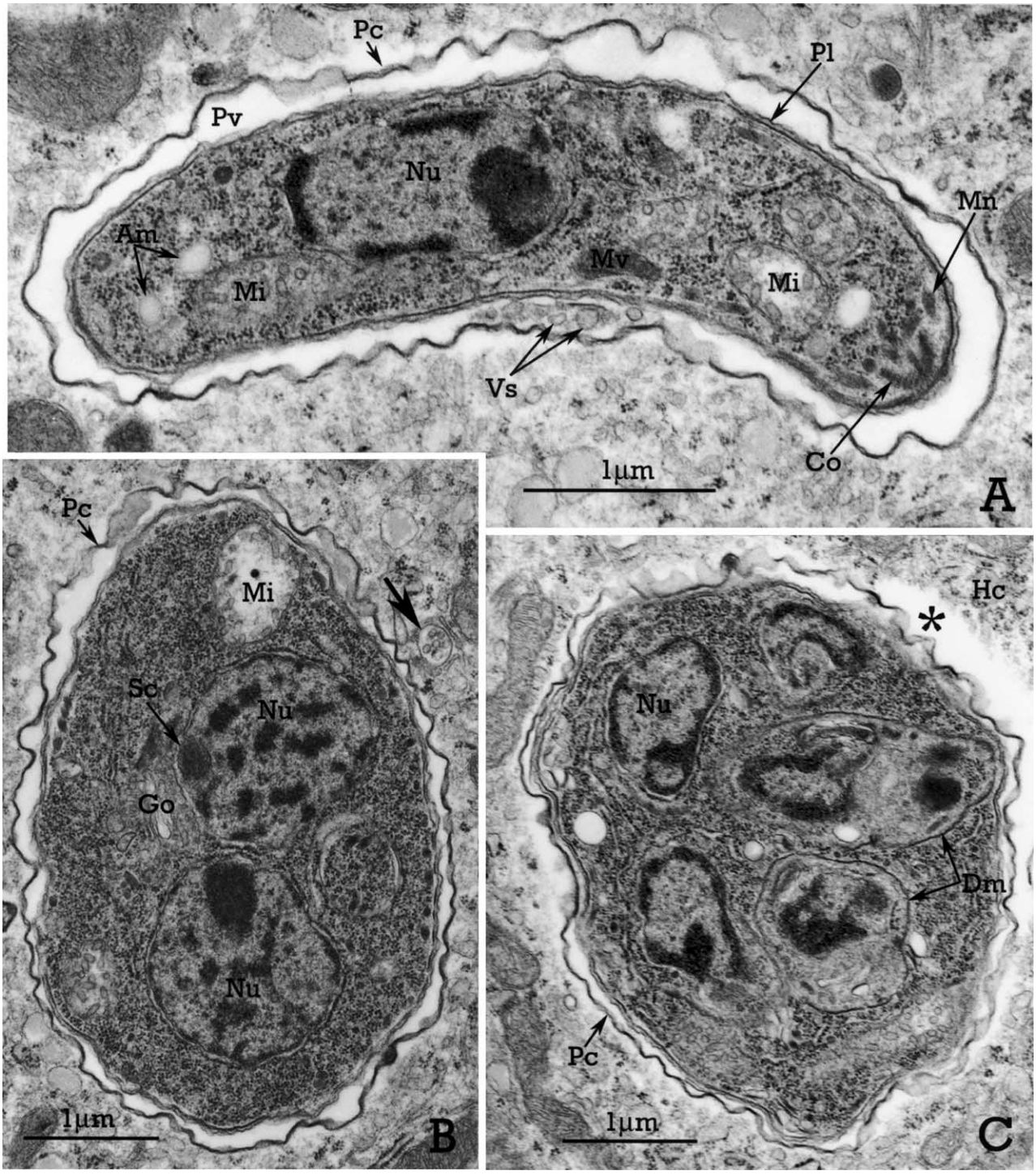

Fig. 5. Transmission electron micrographs of developmental stages of type D schizonts; 46 h p.i. (A) Type C merozoite in early stage of transformation to a type D schizont; note merozoite contains several amylopectin granules (Am) and several prominent mitochondria (Mi), and electron-dense, undulating parasitophorous vacuolar membrane complex (Pc) consisting of 2–4 fused membranes; Co, conoid; Mn, microneme; Mv, multiple-membrane bound vacuole; Nu, nucleus of merozoite; Pl, plasmalemma of merozoite; Vs, vesicles in parasitophorous vacuole (Pv). (B) Intermediate type D schizont showing two nuclei (Nu); Go, Golgi complex; Mi, mitochondrion; Pc, parasitophorous vacuolar membrane complex; Sc, spindle polar cone; arrow points to host cell vacuole containing several small vesicles. (C) Schizont showing merozoites developing (Dm) by endopolygeny; note space (*) between host cell cytoplasm (Hc) and the parasitophorous vacuolar membrane complex (Pc).

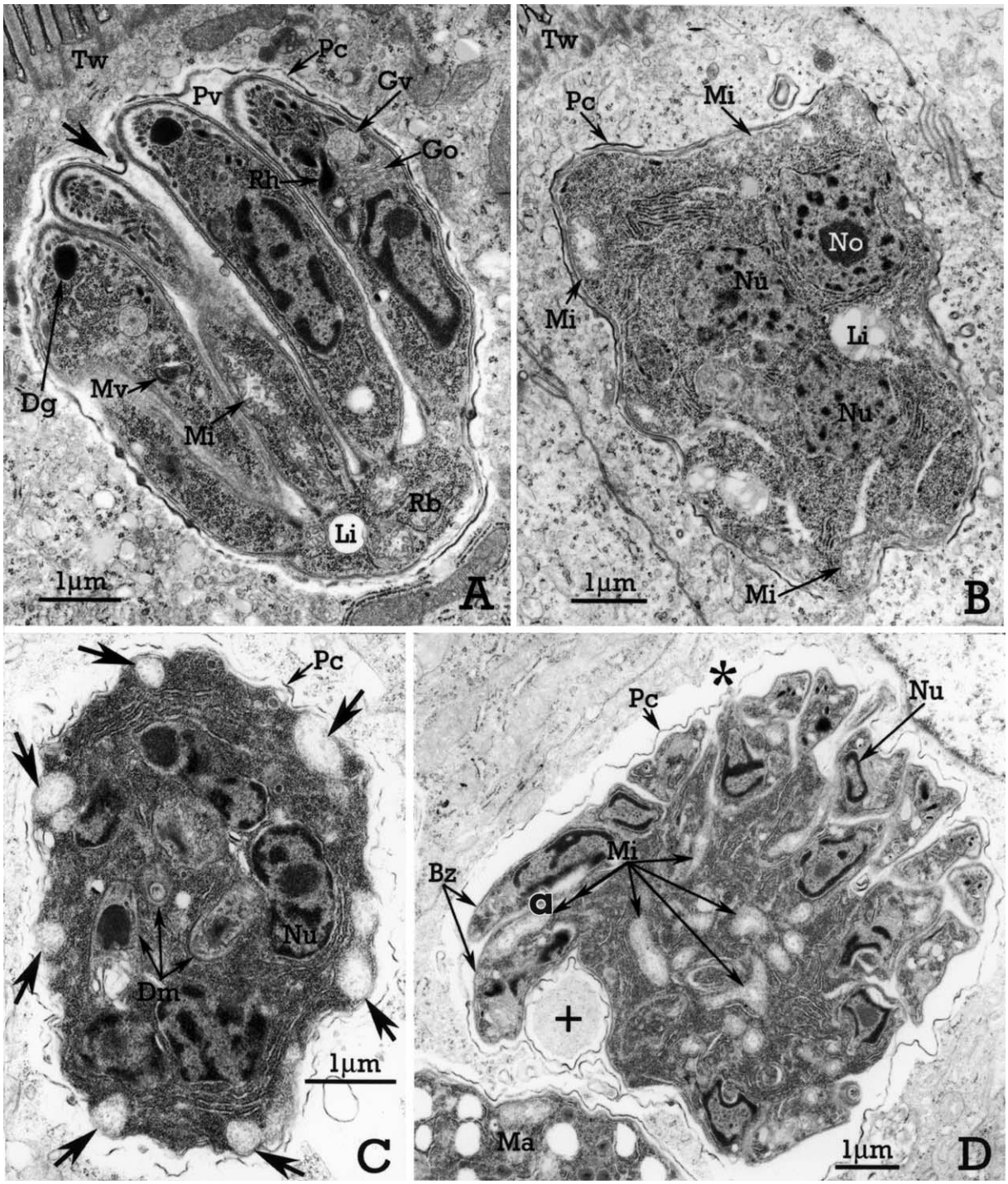

Fig. 6. Transmission electron micrographs of type D (A) and E (B–D) schizonts in enterocytes. (A) Type D schizont with merozoites budding from a residual body (Rb). Merozoites show a prominent vacuole (Gv) containing granular material immediately above maturation face of Golgi complex, electron-dense rhoptries (Rh) and large mitochondria (Mi); the parasitophorous vacuolar membrane complex (Pc) is indented between two merozoites (arrow); Dg, dense granule; Li, lipid body; Mv, multiple-membrane bound vacuole; Pv, parasitophorous vacuole; Tw, terminal web of enterocyte; 46 h p.i. (B) Intermediate type E schizont showing angular shape, numerous mitochondria (Mi) immediately beneath the surface of the schizont, and several lipid bodies (Li); schizont is surrounded by a characteristic parasitophorous vacuolar membrane complex (Pc); No, nucleolus; Nu, nucleus; Tw, terminal web of enterocyte; 6 days p.i. (C) Type E schizont in early stage of merozoite development (Dm) by endopolygeny; note characteristic angular shape of schizont and mitochondria (arrows) located immediately beneath the pellicle of the parasite; Nu, nucleus; Pc, parasitophorous vacuolar membrane complex; 6 days p.i. (D) Type E schizont with budding merozoites (Bz); note numerous mitochondria (Mi) one of which (a) has been incorporated into a budding merozoite, the large vacuole (+) containing fine granular material within the parasitophorous vacuole, and the space between the host cell cytoplasm and the parasitophorous vacuolar membrane complex (Pc); a portion of a macrogamont (Ma) is visible at the lower left; Nu, nucleus of budding merozoite; 4 days p.i.

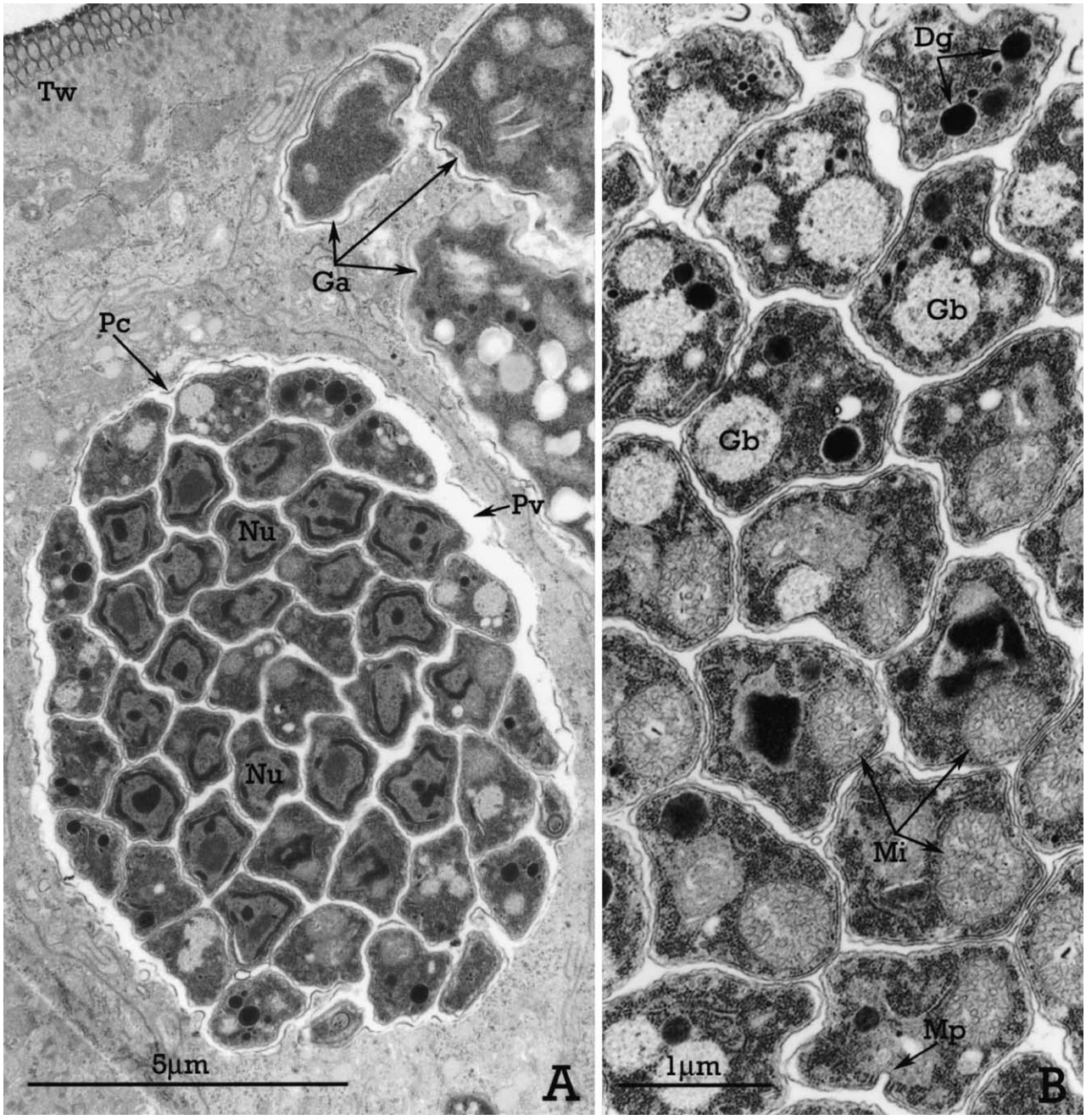

Fig. 7. Transmission electron micrographs of type E schizonts and merozoites in enterocytes; 4 days p.i. (A) Mature type E schizont showing approximately 50 merozoites; Ga, gamonts; Nu, nucleus of merozoite; Pc, parasitophorous vacuolar membrane complex; Pv, parasitophorous vacuole; Tw, terminal web of enterocyte. (B) Type E merozoites showing large mitochondria (Mi) and characteristic granular bodies (Gb); Dg, dense granules; Mp, micropore.

approximately 2–3 μm in diameter and contained residual mitrochondria, ribosomes, endoplasmic reticula and amylopectin granules (Fig. 4B).

The PV surrounding mature schizonts contained small clusters of granular material (Fig. 4C), no TMN, and the PVM was closely associated with the pellicle of the merozoites. Merozoites had a wavy plasmalemma, a nucleus located in the posterior one half of the merozoite, one or two prominent mitochondria, electron-dense rhoptries, and amylopectin granules, most of which were located in the posterior one half of the merozoite (Fig. 4C). Merozoites measured 6.1×1.5 μm ($n = 10$) in size.

3.2.3. Type D schizonts

Type C merozoites apparently developed into type D schizonts within enterocytes or intraepithelial lymphocytes (Figs. 5A–C and 6A). Single, type C merozoites were located within a prominent PV characterised by a wavy,

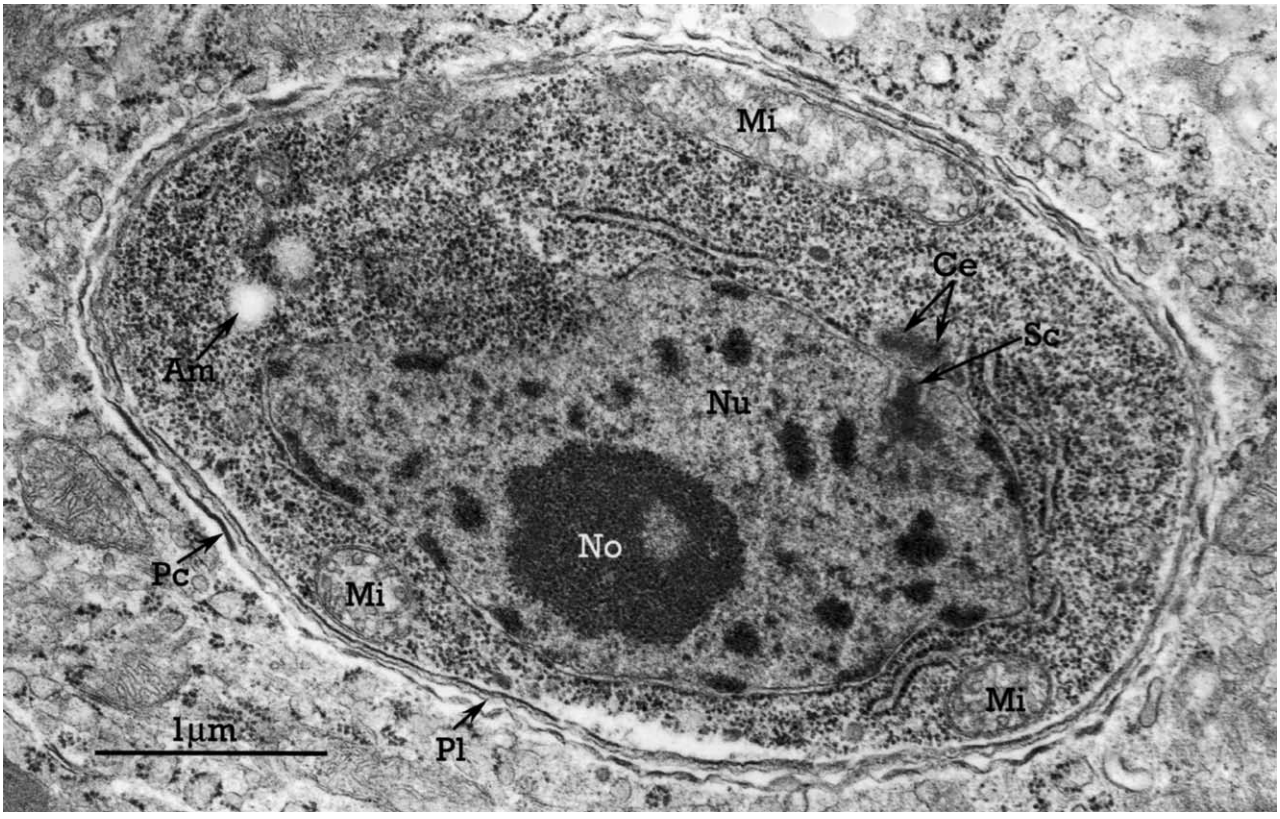

Fig. 8. Transmission electron micrographs of a uninucleate organism probably of an early microgamont showing nucleus in early stage of nuclear division with spindle polar cone (Sc) and centrioles (Ce); Am, amylopectin; Mi, mitochondria; No, nucleolus; Nu, nucleus; Pc, parasitophorous vacuolar membrane complex; plasmalemma of microgamont; 6 days p.i.

electron-dense PVM complex consisting of two to four fused membranes (Fig. 5A). Except for a few clusters of spherical vesicles, the PV was homogenously electron-lucent (Fig. 5A). After several nuclear divisions, 12–18 merozoites developed by endopolygeny (Figs. 5B, C and 6A), eventually budding from a laterally located residual body (Fig. 6A). Characteristic ultrastructural features of type D merozoites included electron-dense rhoptries and a vacuole, 400–450 nm in diameter, filled with granular material, located immediately above the Golgi complex (Fig. 6A). Mature merozoites often indented the PVM (Fig. 6A). Merozoites measured 5.8×1.3 μm ($n=10$) in size.

3.2.4. Type E schizonts

Type E schizonts appeared to arise from type D merozoites that escaped into neighboring cells and underwent endopolygeny as described for type C and D schizonts (Figs. 6B–D, and 7A and B). Although they shared many ultrastructural characteristics with earlier stages including an electron-dense PVM complex, type E schizonts and merozoites could be distinguished from types C and D. Early and advanced intermediate schizonts were usually angular in appearance and had numerous, prominent mitochondria situated immediately beneath the pellicle (Fig. 6B and C). During late endopolygeny, merozoites budded from a centrally located residual body at the schizont surface to form 50–80 tightly packed, merozoites (Figs. 6D, and 7A and B). Type E merozoites had electron-dense rhoptries, one or two large mitochondria and several granular bodies, 300–600 nm in diameter, that appeared similar to the granular vacuole in type D merozoites, except that the granular body was not surrounded by a membrane (Fig. 7B). Type E merozoites measured 4.5×1.1 μm ($n=10$) in size.

3.3. Gamonts and oocysts

Gamonts and oocysts were present at 4 and 6 days p.i. and developed exclusively within enterocytes; none were seen in intraepithelial lymphocytes. Gamonts and oocysts were surrounded by an electron-dense PVM complex similar to those surrounding types D and E schizonts (Figs. 8, 9A and 10). Even though micro- and macrogamonts developed in close proximity to type E schizonts (Fig. 7A), it was not possible to determine which merozoite types gave rise to gamonts.

Large forms measuring 5.7×3.5 μm ($n=10$) in size and containing a large nucleus with a prominent nucleolus undergoing nuclear division were considered to be early microgamonts (Fig. 8). After several nuclear

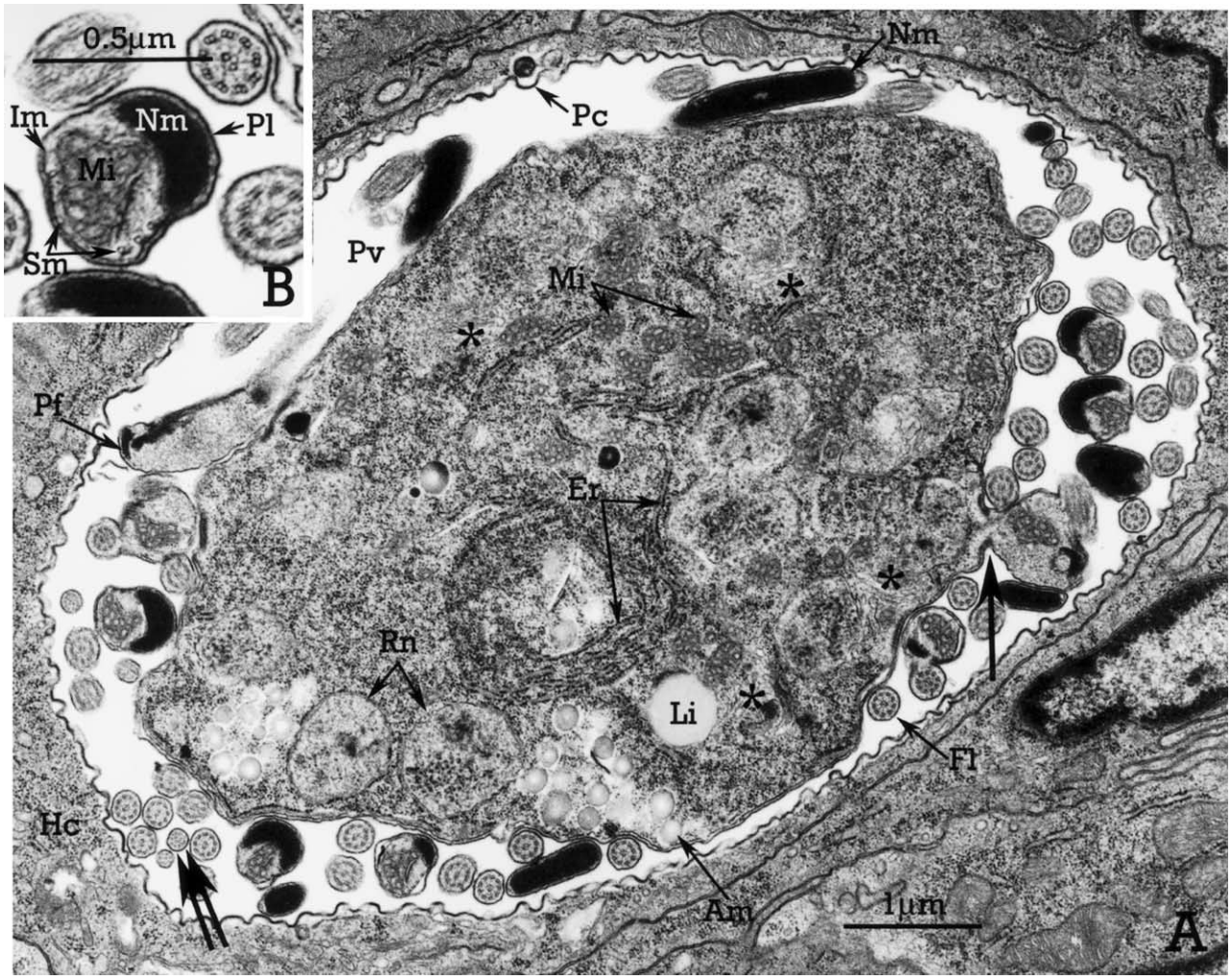

Fig. 9. Transmission electron micrographs of a mature microgamont; 6 days p.i. (A) Microgamont with microgametes budding at the surface (arrow); microgamete flagellum (Fl) contain typical 9+2 microtubules except at the flagellar tips (double arrow) where the microtubules are arranged singularly; residual body contains numerous amylopectin granules (Am), Golgi complexes (*), mitochondria (Mi), residual nuclei (Rn), endoplasmic reticulum (Er) and lipid bodies (Li); Hc, host cell cytoplasm; Nm, electron-dense nucleus of microgamete; Pc, parasitophorous vacuolar membrane complex; Pf, perforatorium of microgamete; Pv, parasitophorous vacuole. (B) Higher magnification of cross section of microgamete in (A) showing inner membrane complex (Im) and subpellicular microtubules (Sm) in region near mitochondrion (Mi); Nm, nucleus of microgamete; Pl, plasmalemma of microgamete.

divisions, nuclei were situated near the margin of the gamont and microgametes budded from the surface leaving behind a large residual body containing various organelles and inclusion bodies including electron-lucent residual nuclei, amylopectin granules, Golgi complexes, endoplasmic reticula, multiple membrane bound vacuoles, mitochondria and numerous ribosomes (Fig. 9A). Microgametes were biflagellate and contained a perforatorium, two flagella that arose from two basal bodies immediately behind the perforatorium, a single mitochondrion, an electron-dense nucleus, and an inner membrane complex associated with approximately 12 microtubules. The inner membrane complex and subpellicular microtubules occurred in the region immediately above the mitochondrion but were absent in the region near the microgamete nucleus (Fig. 10B). The PV surrounding microgamonts was filled with a clear electron-lucent material (Fig. 10A).

Mature macrogametes measured 8.1×6.0 µm ($n = 10$) in size and contained all the organelles and inclusion bodies characteristically found in those of other coccidia. Type I wall-forming bodies arose from the maturation forming face of the Golgi complexes, whereas type II wall-forming bodies developed within the cisterna of the endoplasmic reticulum connected to the forming face of the Golgi complex (Fig. 10A). Type I wall forming bodies were electron-dense, whereas type II bodies had an electron-dense core and a moderately dense margin. The PV was filled with a finely granular, moderately electron-dense material and contained a few vacuoles with granular material surrounded by membranes similar to those of the PVM complex (Fig. 10A).

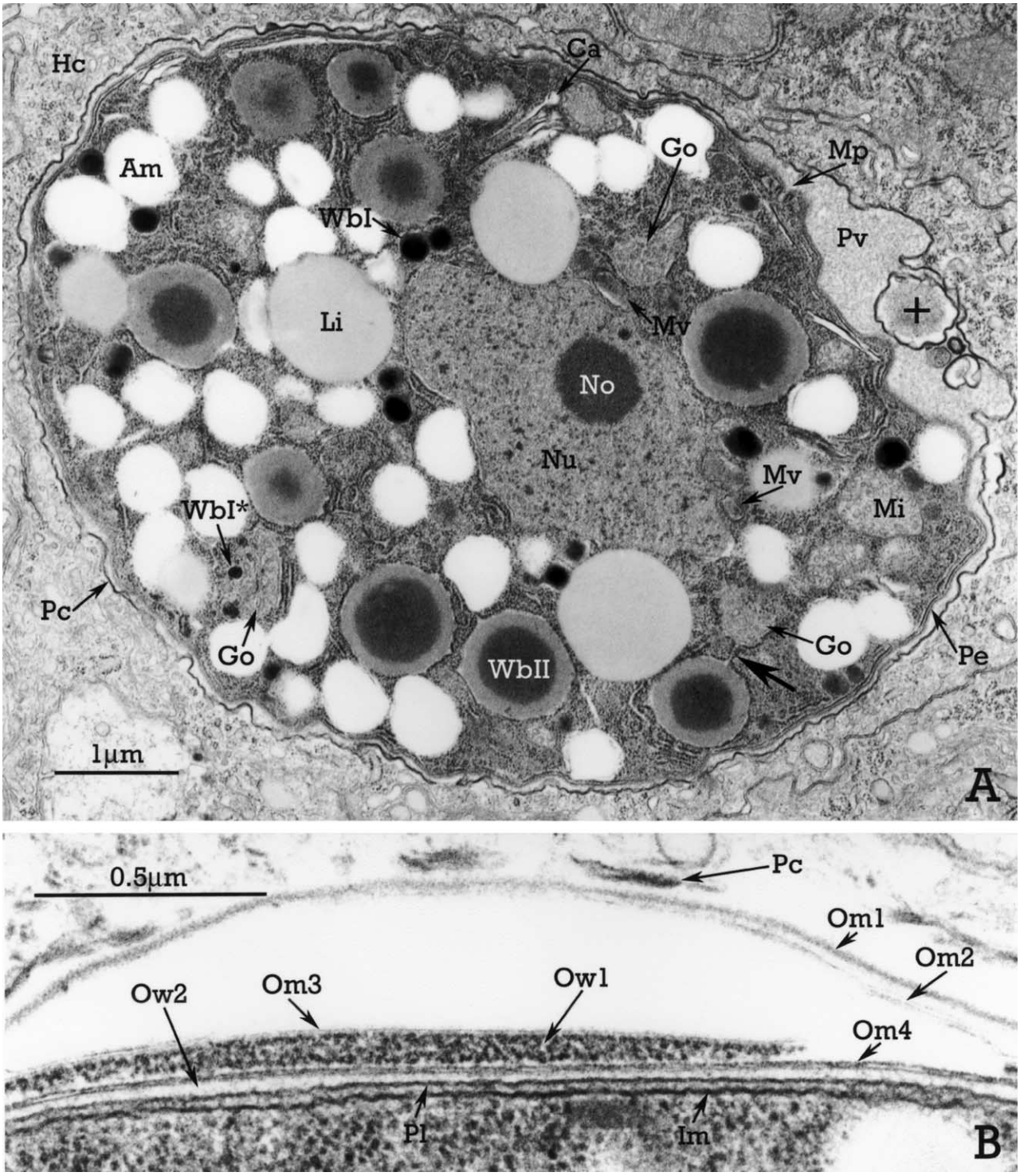

Fig. 10. Transmission electron micrographs of a mature macrogamont (A) and an early stage of oocyst wall formation (B). (A) Mature macrogamont showing characteristic canaliculi (Ca), wall forming bodies I and II (WbI, WbII), lipid bodies (Li), amylopectin granules (Am) and centrally located nucleus (Nu) with prominent nucleolus (No); pellicle (Pe) consists of plasmalemma and inner membrane complex; note large vacuole (+) with granular material within the parasitophorous vacuole (Pv); and wall forming body I (wbI*) forming at maturation face of Golgi complex; Go, Golgi complex; Hc, host cell cytoplasm; Mi, mitochondrion; Mp, micropore; Mv, multiple membrane bound vacuole; Pc, parasitophorous vacuolar membrane complex; 4 days p.i. (B) High magnification of surface of zygote with developing oocyst wall; portions of the parasitophorous vacuolar membrane complex (Pc) have disappeared; the outer layer of the oocyst wall (Ow1) is forming between membranes 3 (Om3) and 4 (Om4) and the inner layer (Ow2) is beginning to form between the plasmalemma (Pl) of the zygote and membrane 4 (Om4); Im, inner membrane complex of pellicle; 6 days p.i.

Table 1
Ultrastructural differentiation of tachyzoites and types B–E schizonts and merozoites of *Toxoplasma gondii* in the small intestine of cats fed bradyzoites

Characteristic	Parasite or schizont Type				
	Tachyzoites	B	C	D	E
Location	Lamina propria	Epithelium, lamina propria	Epithelium, lamina propria	Epithelium	Epithelium
Division	Endodyogeny, asynchronous	Endodyogeny, asynchronous	Endopolygeny, synchronous	Endopolygeny, synchronous	Endopolygeny, synchronous
Parasitophorous vacuole					
TMN	Present	Present	Absent	Absent	Absent
PVM	Thin	Thin	Thin	Thick	Thick
Granular material	Absent	Absent	Present	Absent	Absent
Residual body	Absent	Absent	Present	Present	Present
Schizont size, number measured		26×17 μm, 10	16×10 μm, 8	7.3×5.6 μm, 6	12×8.8 μm, 10
Number of merozoites per schizont		2–48	24–36	12–18	50–80
Tachyzoites or merozoites					
Size, number measured	4.7×2.1 μm, 10	5.8×2.9 μm, 10	6.1×1.5 μm, 8	5.8×1.3 μm, 10	4.5×1.1 μm, 10
Amylopectin	Few	Few	Several	Few	Few
Rhoptries	Labyrinthine	Labyrinthine	Electron-dense	Electron-dense	Electron-dense
Granular vacuole	Absent	Absent	Absent	Present	Absent
Granular body	Absent	Absent	Absent	Absent	Present

Only the early stages of oocyst wall formation were observed because preparation artifacts precluded observation of the later stages. During early wall formation, four membranes (Om1 to Om4) appeared at the surface of the oocyst external to the parasite pellicle (Fig. 10B). The outer layer of the oocyst wall formed between membranes Om3 and Om4; the inner layer formed between Om4 and the plasmalemma of the sporont (Fig. 10B). When the layers of the oocyst wall began to form, segments of the PVM complex disappeared (Fig. 10B). The outer layer of the oocyst wall was electron-dense; the inner layer moderately electron-dense (not shown).

4. Discussion

Dubey and Frenkel (1972) structurally distinguished five types of *T. gondii* in the intestine of cats fed tissue cysts. Type A was the first divisional stage in enterocytes and was seen at 12 h p.i.; we did not find this stage in the present study because five cats were euthanised 24 h p.i. In the sixth cat euthanised 8 h p.i. only individual zoites, probably bradyzoites, were seen. By light microscopy, types B and C found in the present study were identical to those described by Dubey and Frenkel (1972). Dubey and Frenkel (1972) distinguished type D schizonts from type E based on the presence of a residual body in type E and its absence in type D. However, results of the present study indicate that both types D and E can have residual bodies but their merozoites are different in size and number per schizont. Both types D and E schizonts are enclosed in one type of PV with a thick vacuolar membrane complex and no TMN. Ferguson and Wright (1998) and Ferguson (2004) reported a thick PV consisting of three fused membranes surrounding schizonts and gamonts of *T. gondii*. In our study, the PV surrounding types D and E schizonts and gamonts had a thick PV consisting of two to four fused electron-dense membranes, whereas type B and C schizonts had a single PV membrane. Since Ferguson and Wright (1998) and Ferguson (2004) examined tissues fixed at day 7 p.i., they missed types B and C schizonts. In addition, we found that type B schizonts had an extensive TMN and type C schizonts had no TMN. Distinguishing features of type B, C, D and E schizonts and merozoites are summarised in Table 1. Typically, in all coccidian schizonts, including those in *Hammondia hammondi* schizonts are enclosed in PV that lack TMN (Dubey and Sreekumar, 2003).

In the present study, individual type B merozoites and multinucleated structures were found in the same PV. A similar phenomenon has been observed in *Isospora felis* and *Isospora rivolta* of cats (Shah, 1971; Dubey, 1979). Ferguson et al. (1980) reported that the division of one type of *I. felis* schizonts in feline enterocytes by endodyogeny was identical to that observed in *T. gondii* tachyzoites. In the present study, we were unable to study differentiation of the merozoites from these multinucleated forms. Therefore, we are uncertain whether these multinucleated forms were early type C or gave rise to type B. Coccidian schizonts typically develop in enterocytes although sporozoites can be transported by intraepithelial lymphocytes. In the present study, Type B and C schizonts matured in intraepithelial lymphocytes.

Our results confirm the findings of Ferguson et al. (1975) regarding the development of macrogamonts and

oocysts and provide additional details concerning microgametogenesis. For example, we found that during early development the nucleus divides into two, four and then multiple nuclei, which become located peripherally and amylopectin is centrally located. By light microscopy, intermediate microgamonts are periodic acid Schiff (PAS)-positive because of the amylopectin. Even in the absence of flagella the nuclei in microgamonts at the 8–10 nucleated stage are smaller in size than the nuclei of schizonts (Dubey and Frenkel, 1972). They also show changes in chromatin distribution not seen in developing schizonts (Ferguson et al., 1974).

The wall forming bodies (WB) in the present study were different from those reported earlier for *T. gondii*. The WBI were electron-dense, and similar to that reported by Ferguson et al. (1975) but denser than those reported by Pelster and Piekarski (1972). We also found that WBI developed at the maturation face of the Golgi complex, whereas WBII developed within the cisterna of the rough endoplasmic reticulum connected to the forming face of the Golgi complex. In the present study, WBII had an electron-dense core and a moderately electron-dense outer margin, thus differing from the homogeneous structures of WBII reported by Ferguson et al. (1975). These differences might have resulted from enzymes acting on the WBII to mobilise components to form the layers of the oocyst wall or from differences in fixation and processing of specimens.

References

Cornelissen, A.W.C.A., Overdulve, J.P., Hoenderboom, J.M., 1981. Separation of *Isospora* (*Toxoplasma*) *gondii* cysts and cystozoites from mouse brain tissue by continuous density-gradient centrifugation. Parasitology 83, 103–108.

Dubey, J.P., 1879. Life cycle of *Isospora rivolta* (Grassi, 1879) in cats and mice. J. Protozool. 26, 433–443.

Dubey, J.P., 1995. Duration of immunity to shedding of *Toxoplasma gondii* oocysts by cats. J. Parasitol. 81, 410–415.

Dubey, J.P., 1996. Infectivity and pathogenicity of *Toxoplasma gondii* oocysts for cats. J. Parasitol. 82, 957–960.

Dubey, J.P., 2001. Oocyst shedding by cats fed isolated bradyzoites and compariosion of infectivity of bradyzoites of the VEG strain *Toxoplasma gondii* to cats and mice. J. Parasitol. 87, 215–219.

Dubey, J.P., Frenkel, J.K., 1972. Cyst-induced toxoplasmosis in cats. J. Protozool. 19, 155–177.

Dubey, J.P., Frenkel, J.K., 1976. Feline toxoplasmosis from acutely infected mice and the development of *Toxoplasma* cysts. J. Protozool. 23, 537–546.

Dubey, J.P., Sreekumar, C., 2003. Redescription of *Hammondia hammondi* and its differentiation from *Toxoplasma gondii*. Int. J. Parasitol. 33, 1437–1453.

Dubey, J.P., Lunney, J.K., Shen, S.K., Kwok, O.C.H., Ashford, D.A., Thulliez, P., 1996. Infectivity of low numbers of *Toxoplasma gondii* oocysts to pigs. J. Parasitol. 82, 438–443.

Ferguson, D.J.P., 2004. Use of molecular and ultrastructural markers to evaluate stage conversion of *Toxoplasma gondii* in both the intermediate and definitive host. Int. J. Parasitol. 34, 347–360.

Ferguson, D.J.P., Wright, S.E., 1998. An ultrastructural study of the host/parasite relationship of *Toxoplasma gondii* during enteric development in the small intestine of the cat. Electron Microscopy 4, 335–336.

Ferguson, D.J.P., Hutchison, W.M., Dunachie, J.F., Siim, J.C., 1974. Ultrastructural study of early stages of asexual multiplication and microgametogony of *Toxoplasma gondii* in the small intestine of the cat. Acta Pathol. Microbiol. Scand. B 82, 167–181.

Ferguson, D.J.P., Hutchison, W.M., Siim, J.C., 1975. The ultrastructural development of the macrogamete and formation of the oocyst wall of *Toxoplasma gondii*. Acta Pathol. Microbiol. Scand. B 83, 491–505.

Ferguson, D.J.P., Birch-Andersen, A., Hutchinson, W.M., Siim, J.C., 1980. Ultrastructural observations showing enteric multiplication of *Cystoisospora* (*Isospora*) felis by endodyogeny. Z. Parasitenk. 63, 289–291.

Frenkel, J.K., Dubey, J.P., Miller, N.L., 1970. *Toxoplasma gondii* in cats: fecal stages identified as coccidian oocysts. Science 167, 893–896.

Freyre, A., Dubey, J.P., Smith, D.D., Frenkel, J.K., 1989. Oocyst-induced *Toxoplasma gondii* infections in cats. J. Parasitol. 75, 750–755.

Hutchison, W.M., Dunachie, J.F., Work, K., Siim, J.C., 1971. The life cycle of the coccidian parasite, *Toxoplasma gondii*, in the domestic cat. Trans. Roy. Soc. Trop. Med. Hyg. 65, 380–399.

Overdulve, J.P., 1978. Studies on the life cycle of *Toxoplasma gondii* in germfree, gnotobiotic and conventional cats (I). Proc. Kon. Ned. Akad. Wet. C 81, 19–32.

Pelster, B., Piekarski, G., 1972. Untersuchungen zur Feinstruktur des Makrogameten von *Toxoplasma gondii*. Z. Parasitenk. 39, 225–232.

Piekarski, G., Pelster, B., Witte, H.M., 1971. Endopolygenie bei *Toxoplasma gondii*. Z. Parasitenk. 36, 122–130.

Shah, H.L., 1923. The life cycle of *Isospora felis*, Wenyon, 1923 a coccidium of the cat. J. Protozool. 18, 3–17.

Sheffield, H.G., 1970. Schizogony in *Toxoplasma gondii*: an electron microscope study. Proc. Helminthol. Soc. Wash. 37, 237–242.

Speer, C.A., Dubey, J.P., Blixt, J.A., Prokop, K., 1997. Time-lapse video microscopy and ultrastructure of penetrating sporozoites, types 1 and 2 parasitophorous vacuoles, and the VEG strain of *Toxoplasma gondii*. J. Parasitol. 83, 565–574.